IEEE Access
Multidisciplinary | Rapid Review | Open Access Journal

Received January 30, 2020, accepted February 14, 2020, date of publication February 17, 2020, date of current version March 3, 2020.

Digital Object Identifier 10.1109/ACCESS.2020.2974526

MLP-Based Neural Guaranteed Performance Control for MEMS Gyroscope With Logarithmic Quantizer

HAONAN SI[1,3], XINGLING SHAO[1,2], AND WENDONG ZHANG[1,2]

[1]Key Laboratory of Instrumentation Science and Dynamic Measurement, Ministry of Education, North University of China, Taiyuan 030051, China
[2]National Key Laboratory for Electronic Measurement Technology, North University of China, Taiyuan 030051, China
[3]School of Information and Communication Engineering, North University of China, Taiyuan 030051, China

Corresponding author: Xingling Shao (huanying3557913@sina.com)

This work was supported in part by the National Natural Science Foundation of China under Grant 61603353 and Grant 61803348, in part by the Fund for the Shanxi 1331 Project Key Subjects Construction under Grant 1331KSC, in part by the Shanxi Province Science Foundation for Youths under Grant 201701D221123, and in part by the Scientific and Technological Innovation Programs of Higher Education Institutions in Shanxi.

ABSTRACT In this paper, a minimum-learning-parameter (MLP) based neural control method is proposed for micro-electro-mechanical system (MEMS) gyroscope with prescribed performance and input quantization. For the first time, a logarithmic quantizer (LQ) is employed to generate smooth input control signal for MEMS gyroscope, which greatly reduces the communication data size as well as actuator bandwidth. To improve the performance of MEMS gyroscope in the presence of quantization error, a prescribed performance control scheme consisting of preselected performance boundaries and an error transformation is utilized, such that preselected transient and steady-state properties can be assured. In contrast to the neural control strategies subject to the issue of learning explosion, a MLP-based neural network (NN) is introduced to estimate the unknown uncertainties using the norm of neural weight. To eliminate the effect of quantization error induced by LQ, a robust quantized control is designed to further ensure the closed-loop system suffering from discontinuous dynamics with prescribed ultimately uniformly bounded (UUB) performance. In the end, a series of simulations are presented to validate the superiority of the proposed control methodology.

INDEX TERMS MEMS gyroscope, logarithmic quantizer, minimum-learning-parameter, prescribed performance control.

I. INTRODUCTION

As an efficient angular rate sensor, micro-electro-mechanical system (MEMS) gyroscope is extensively utilized in inertial navigation, consumer electronics, automobile and even national defense industry by virtue of its remarkable advantages over traditional ones, especially its tiny size, easy integration, higher energy efficiency and availability of mass production [1]–[3]. Commonly, to obtain the precise information of MEMS gyroscope in terms of rotation rate, fast and accurate tracking of the reference trajectory is of high priority. However, in industrial application, diverse operating situations of MEMS gyroscope inevitably induce unknown external disturbances, which typically degrades the control performance. What is more, the parametric uncertainties and couplings between drive and sense modes resulting from fabrication flaws further render the MEMS gyroscope having uncertain dynamics and as a consequence, the measuring accuracy of angular rate is unavoidably decreased. Hence, it is of great significance to design an elegant control method for MEMS gyroscope in pursuit of higher measuring accuracy.

Focusing on raising the measuring accuracy of MEMS gyroscope, tremendous advanced control schemes have been proposed, such as sliding-mode control [4]–[6], fuzzy logic control [5], [7], robust and adaptive control [7], [8], as well as neural networks (NNs) [6], [9]. As an example, in [7], the backstepping control, where the controller design contains several steps and, in each step, the virtual control law is recursively designed such that the ultimately uniformly bounded (UUB) properties of MEMS gyroscope can be

The associate editor coordinating the review of this manuscript and approving it for publication was Nasim Ullah.

achieved. In [8], to deal with the issue of term explosion arising from multiple differentiating, the dynamic surface control (DSC) is explored, where a first-order low-pass filter is applied to approximate the time derivative of virtual control signal and meanwhile, NNs are employed to online identify the unknown dynamics by virtue of their universal approximation, such that, the robustness against uncertainties of MEMS gyroscope is greatly improved. Despite the fact that available works [4]–[9] for MEMS gyroscope are of great superiority, it is worth pointing out that almost all of them are subject to the following two serious problems. One is concerned with bandwidth restriction of actuator, i.e., the existing results for MEMS gyroscope are almost achieved under the unpractical assumption that the actuator of MEMS gyroscope can perform with arbitrarily high precision and the capacity of communication channel from control module to actuator is large enough to transmit continuous signal with infinite accuracy, which is in contradiction with the physical truth of MEMS gyroscope. Another problem is that although previous works can realize remarkable closed-loop stability with UUB properties, the upper bound of final tracking error cannot get rid of the heavy dependence on unknown disturbances and as a consequence, in pursuit of guaranteed performance in terms of tracking accuracy, controller parameters are always required to be repeatedly tuned and some design conservatism is introduced. Therefore, how to design an advanced control methodology for MEMS gyroscope considering input quantization and predetermined performance is still an open issue and deserves deep study.

Quantization, a ubiquitous process in modern digital communication, refers to the conversion of continuous signal to the one with finite-precision via mapping from infinite sets to finite sets. With the aid of quantization, the control signal can be transmitted over a constrained communication channel, performed with a limited digital microprocessor while the normal operation of system will not be influenced. Enlightened by the quantization in communication systems, researchers are more and more focused on quantized control of uncertain systems subject to input quantization. Logarithmic quantizer (LQ) [10], [11], one of the most employed quantizers in digital communication systems, can largely reduce the communication data size and meanwhile, it is capable of generating quantized signals with constant quantization signal-to-noise ratio (SNR) owing to its exponentially transformed quantization levels compared with uniform quantizer (UQ) [12], such that the robustness of system will not change along with the variation of control signal magnitude. Nevertheless, the introduction of input quantization typically induces unexpected quantization error, which will inevitably influence the tracking accuracy of MEMS gyroscope, while to the best of authors' knowledge, how to make a compromise between the tracking performance and bandwidth restriction is rarely studied in existing results [4]–[9]. Thus, it is an urgent and tough issue to eliminate the influence of quantization error and guarantee high-accuracy tracking performance for MEMS gyroscope in the existence of quantized input.

To further improve the tracking performance in both transient and steady-state phases and remove the design conservatism universally existing in previous control methods for MEMS gyroscope, which can only ensure the closed-loop stability with UUB, prescribed performance control (PPC) proposed in [13]–[15] is an efficient strategy. Nowadays, PPC has been commonly used in uncertain nonlinear systems such as air-breathing hypersonic vehicle (AHV) [16], [17] and [35], robotic manipulator [13] and underwater vehicles [18]. With the aid of a proper equivalent error transformation function, PPC can assure the tracking error within predetermined boundaries, such that the prescribed performance can be realized without the tedious tuning of design parameters. For instance, within the framework of the controller design for backstepping, the PPC methodology in [19] is capable of realizing the tracking of both velocity and altitude with prescribed performance for AHV. However, the analytical differentiating of virtual control law inevitably leads to the issue of differentiating explosion, which may further affect the normal operation of controller. To eliminate this obstacle, dynamic surface control (DSC) [20], [21] is usually combined with PPC, where a first-order low-pass filter is employed to approximate the time derivative of virtual control signal. However, to the best of authors' knowledge, the available PPC studies are typically designed for actuator with arbitrarily high performing accuracy, which is not feasible for algorithm implementation in digital microprocessor of MEMS gyroscope.

In light of the manufacturing defects and diverse working conditions of MEMS gyroscope, its measuring accuracy is typically affected by uncertainties containing external disturbances, parametric uncertainties and coupling between two operation modes. Hence, the accurate identification of lumped disturbances directly determines the performance of MEMS gyroscope. Under such circumstances, neural networks (NNs) are widely employed to online identify unknown disturbances for uncertain systems [22]–[24] by virtue of their universal approximation. However, the complex structure of NN unavoidably induces heavy computational load, such that an unexpected time delay may be introduced to controller, which can further result in poor transient performance especially under some fast time-varying measuring conditions. Thus, how to avoid the problem of learning explosion without degrading the identification accuracy is of great urgency and necessity.

To solve the issues mentioned above, a MLP-based neural guaranteed performance control for MEMS gyroscope with logarithmic quantizer is proposed and its superiorities over available studies are collected in TABLE 4 in APPENDIX, which can be summarized as follows:

- Different from the available works [4]–[9] under the unpractical hypotheses that the actuator can perform with arbitrarily high accuracy and data transmission

from control module to actuator can be realized via unlimited communication channel, LQ is firstly employed to generate finite-precision input control signal for MEMS gyroscope that possible digital controller can be promoted. In addition, different from existing quantization error decomposition [25], [35] relying on the control input to be bounded, which is hard to ensure before the controller design, a novel quantization decomposition approach is investigated for MEMS gyroscope to relax such condition and guarantee closed-loop stability. Furthermore, PPC technique is explored in controller design in the existence of input quantization to assure both transient and steady-state tracking performance within preselected performance boundaries. Hence, a compromise between the tracking performance of MEMS gyroscope and bandwidth restriction can be obtained.

- Although most existing works [22]–[24] can realize high-accuracy identification of unknown disturbances by means of universal approximation of NNs, it is worth pointing out that almost all of them suffer from the problem of learning explosion. Inspired by the minimum-learning-parameter (MLP) technique in [26], [27] and [36], we employ MLP to reconstruct the lumped disturbances consisting of external disturbances, parametric uncertainties and coupling between two operation modes, which greatly reduces learning dimension, such that the computational load is remarkably eased without decreasing the identification accuracy. What's more, the application of DSC technique effectively eliminates the problem of term explosion caused by analytical differentiation, such that the feasibility of algorithm is notably improved.
- With the aid of Lyapunov stability analysis, the prescribed UUB properties of closed-loop system can be ensured. Extensive simulation results are presented to further validate the effectiveness as well as superiority of the proposed control method.

This rest paper is arranged as follows. The problem formulation and preliminaries will be introduced in Section II. Section III presents the procedure of controller design and section IV proposes the performance analysis. Section V provides a series of simulation results and finally section VI concludes this paper.

II. PROBLEM STATEMENT AND PRELIMINARIES

A. MODELING OF MEMS GYROSCOPE

The schematic diagram of a z-axis vibrational MEMS gyroscope is depicted in Fig. 1 and conventionally, the non-dimension model of MEMS gyroscope, as borrowed form [4], [5], [8], [9], [28] can be formulated as:

$$\begin{cases} \dot{\boldsymbol{x}}_p = \boldsymbol{x}_v \\ \dot{\boldsymbol{x}}_v = \boldsymbol{u} + \boldsymbol{F} \end{cases} \tag{1}$$

where $\boldsymbol{x}_p = [x_{p1}, x_{p2}]^T$ and $\boldsymbol{x}_v = [x_{v1}, x_{v2}]^T$ denote the displacements and velocities of drive and sense mode, respectively. $\boldsymbol{F} = [F_1, F_2]^T$ represents the lumped disturbances, which can be described as

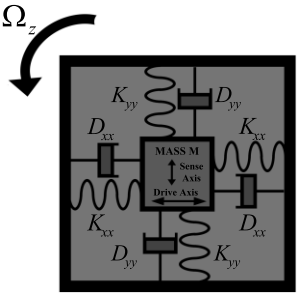

FIGURE 1. Schematic diagram of a z-axis MEMS gyroscope.

$$\boldsymbol{F} = -(\boldsymbol{D} + 2\boldsymbol{\Omega})\boldsymbol{x}_v - \boldsymbol{K}\boldsymbol{x}_p + \boldsymbol{\xi} \tag{2}$$

with

$$\boldsymbol{u} = \begin{bmatrix} u_1 \\ u_2 \end{bmatrix} = \begin{bmatrix} \frac{u_x}{m} \\ \frac{u_y}{m} \end{bmatrix}, \quad \boldsymbol{D} = \begin{bmatrix} \frac{D_{xx}}{m\omega_0} & \frac{D_{xy}}{m\omega_0} \\ \frac{D_{xy}}{m\omega_0} & \frac{D_{yy}}{m\omega_0} \end{bmatrix}$$
$$\boldsymbol{\Omega} = \begin{bmatrix} 0 & -\Omega_z \\ \Omega_z & 0 \end{bmatrix}, \quad \boldsymbol{K} = \begin{bmatrix} \sqrt{\frac{K_{xx}}{m\omega_0^2}} & \frac{K_{xy}}{m\omega_0^2} \\ \frac{K_{xy}}{m\omega_0^2} & \sqrt{\frac{K_{xx}}{m\omega_0^2}} \end{bmatrix} \tag{3}$$

where u_i for $i = 1, 2$ denotes the input signal for MEMS gyroscope and m represents the mass of gyroscope. ω_0 is the reference angular frequency. D_{xx}, D_{yy} and K_{xx}, K_{yy} respectively refer to the uncertain damping coefficients and spring coefficients. K_{xy}, D_{xy} are unknown coupling parameters and ξ is the external disturbances.

Remark 1: It is worth pointing out that the model of MEMS gyroscope mentioned in [4], [5], [8], [9], [28] commonly assume that the input control signal $\boldsymbol{u}$ can be performed with arbitrary accuracy. While in fact, the widespread use of digital microprocessor leads to the fact that most electrostatic actuators of MEMS gyroscope cannot meet such requirement. To break through this restriction, we explore a modified model of MEMS gyroscope as follows.

$$\begin{cases} \dot{\boldsymbol{x}}_p = \boldsymbol{x}_v \\ \dot{\boldsymbol{x}}_v = Q(\boldsymbol{u}) + \boldsymbol{F} \end{cases} \tag{4}$$

where $Q(\boldsymbol{u})$ denotes the quantized control signal generated by LQ, which is formulated as

$$Q(u_i) = \begin{cases} u_{ri}sign(u_i) & \frac{u_{ri}}{1+\eta_i} < |u_i| \le \frac{u_{ri}}{1-\eta_i} \\ 0 & |u_i| \le \frac{u_{mi}}{1+\eta_i}, \quad i = 1, 2 \end{cases} \tag{5}$$

where $u_{ri} = \delta_i^{1-r} u_{mi}$ with integer $r = 1, 2, \ldots, N$, u_{mi} is the smallest quantization level and $\delta_i = (1-\eta_i)/(1+\eta_i)$ is a positive design parameter, which determines the quantization density. Generally speaking, the bigger δ_i is, the more quantization levels will $Q(u_i)$ has and the smoother will quantization

performance be. With the aid of LQ, the input control signal is limited in the finite set of U = $\{\pm u_{ri},0\}$, such that the issue mentioned in *Remark* 1 is eliminated.

The quantized signal $Q(u_i)$ can be considered as the composition of a continuous part and a discontinuous one, which can be described as

$$Q(u_i) = \iota(u_i)u_i + T(u_i) \tag{6}$$

where

$$\iota_i(u_i) = \begin{cases} Q(u_i)/u_i, & Q(u_i) \neq 0 \\ 1, & Q(u_i) = 0, \end{cases}$$
$$T(u_i) = \begin{cases} 0, & Q(u_i) \neq 0 \\ -u_i, & Q(u_i) = 0 \end{cases} \tag{7}$$

Lemma 1 [26]: For $\iota(u_i)$ and $T(u_i)$ in (6), there always exist the following inequalities.

$$1 - \delta_i \leq \iota(u_i) \leq 1 + \delta_i, \quad T(u_i) \leq u_{mi} \tag{8}$$

Assumption 1 [30]: The reference signals x_{pdi}, its time derivative $\dot{x}_{pdi}$, as well as its second derivative with regard to time $\ddot{x}_{pdi}$ for $i = 1, 2$ are commonly considered to be smooth, continuous and bounded functions. Accordingly, we assume a positive constant B_0 belonging to a compact set Ω_0 defined as

$$[x_{pi}^d, \dot{x}_{pi}^d, \ddot{x}_{pi}^d]^T \in \Omega \triangleq \left\{[x_{pi}^d, \dot{x}_{pi}^d, \ddot{x}_{pi}^d]^T : x_{pi}^{d2} + \dot{x}_{pi}^{d2} + \ddot{x}_{pi}^{d2} \leq B_0\right\} \subset \Re^{B_0} \tag{9}$$

Control Objective: Under *assumption*1, for the MEMS gyroscope modeled as (4), our objective is to design a MLP-based neural guaranteed performance control with input quantization to steer position state x_p of MEMS gyroscope to follow the given trajectory. Under the proposed control scheme, the prescribed UUB stability of closed-loop system can be assured and high tracking accuracy are expected.

B. RADIAL BASIS FUNCTION NEURAL NETWORK

In control field, radial basis function neural networks (RBFNNs) are commonly applied to approximate arbitrary unknown continuous function over a compact set $\bar{\boldsymbol{x}}_m \in \Omega \subset \Re^m$ by virtue of its universal approximation [31], [32] and the output of RBFNN can be formulated as

$$y = \omega^T \boldsymbol{h}(\bar{\boldsymbol{x}}_m) \tag{10}$$

where $\boldsymbol{\omega} = [\omega_1, \omega_2, \ldots, \omega_n]^T \in \Re^n, \bar{\boldsymbol{x}}_m = [x_1, x_2, \ldots, x_m]^T \in \Re^m$ respectively denote the weight and input vector. n is the number of neural codes and m represents the input number. $\boldsymbol{h}(\bar{\boldsymbol{x}}_m) = [h_1(\bar{\boldsymbol{x}}_m), h_2(\bar{\boldsymbol{x}}_m), \ldots, h_n(\bar{\boldsymbol{x}}_m)]^T \in \Re^n$ denotes the basis function of RBFNN and it is typically selected as the following Gaussian function formed as

$$h_j(\bar{\boldsymbol{x}}_m) = exp(-\frac{(\bar{\boldsymbol{x}}_m - \boldsymbol{c}_j)^T(\bar{\boldsymbol{x}}_m - \boldsymbol{c}_j)}{b^2}), \quad j = 1, 2, \ldots, n \tag{11}$$

with $\boldsymbol{c}_j = [c_{j1}, c_{j2}, \ldots, c_{jm}]^T \in \Re^m$ and b being the center and width parameter of basis function $h_j(\bar{\boldsymbol{x}}_m)$.

Remark 2: It is notable that the elements of hidden layer will exponentially grow with the increase of learning dimension and based on universal approximation theorem, high-accuracy approximation requires the learning dimension to be large enough, such that high computational burden will be induced to the controller, which will further lead to some severe problems to MEMS gyroscope, especially in some fast time-varying operation environments.

III. CONTROLLER DESIGN

In this section, the proposed control scheme will be elaborated. Its architecture is depicted in Fig. 2 and it is clear that with the aid of proposed PPC, DSC, LQ and MLPNN techniques, fast and high-accuracy tracking of reference trajectory with slight computational burden and limited actuator bandwidth can be realized.

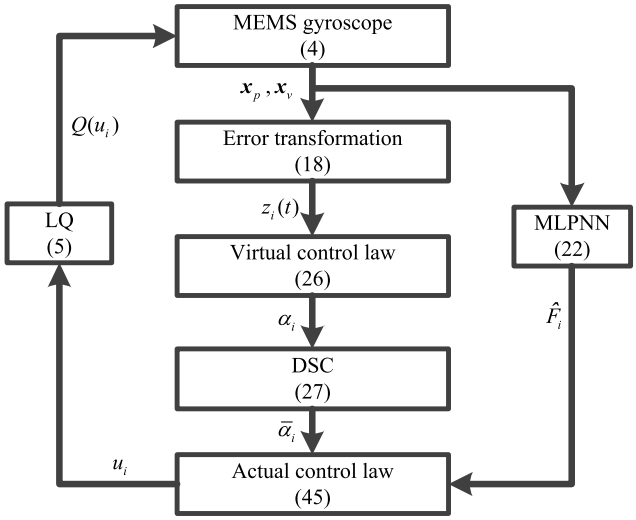

FIGURE 2. Architecture of the proposed algorithm.

A. PRESCRIBED PERFORMANCE CONTROL

Given the dimensionless reference trajectory x_{pd}, the tracking error $\boldsymbol{e}_p = [e_{p1}, e_{p2}]^T$ can be defined as

$$e_{pi}(t) = x_{pi}(t) - x_{pdi}(t) \tag{12}$$

To guarantee the tracking result with prescribed properties, PPC is an efficient approach to improve the tracking performance in both transient and steady-state phases, which can be described as

$$-\epsilon_i \rho_i(t) < e_{pi}(t) < \bar{\epsilon}_i \rho_i(t), \forall t \geq 0 \tag{13}$$

with ϵ_i, $\bar{\epsilon}_i$ being positive constants, $\rho_i(t)$ for $i = 1, 2$ being the preselected performance function and it is typically chosen as the following exponential decaying one [13]–[15].

$$\rho_i(t) = (\rho_{i0} - \rho_{i\infty})e^{-l_i t} + \rho_{i\infty} \tag{14}$$

where ρ_{i0}, $\rho_{i\infty}$, l_i are all positive design parameters and $\rho_{i0} = \rho_i(0)$, $\rho_{i\infty} = \rho_i(\infty)$, such that ρ_{i0} limits the transient overshoots, $\rho_{i\infty}$ ensures the maximum steady-state tracking error and l_i decides convergence rate of performance function $\rho_i(t)$.

Note that it is hard to design control law based on inequality (13), some equivalent error transformation is required to eliminate the time-varying constraints exerted on system states. To facilitate the controller design, the error transformation function $\Theta(z_i(t))$ is introduced to convert constrained error into an unconstrained one and it is formulated as

$$e_{pi}(t) = \Theta(z_i(t))\rho_i(t) \tag{15}$$

with

$$\Theta(z_i(t)) = \frac{\bar{\epsilon}_i \exp(z_i(t)) - \epsilon_i \exp(-z_i(t))}{\exp(z_i(t)) + \exp(-z_i(t))} \tag{16}$$

where $z_i(t)$ is the transformed error. Obviously, $\Theta(z_i(t))$ is a smooth, strictly increasing function and one has

$$\lim_{z_i(t)\to-\infty} \Theta(z_i(t)) = -\epsilon_i, \quad \lim_{z_i(t)\to+\infty} \Theta(z_i(t)) = \bar{\epsilon}_i \tag{17}$$

Following (15), $z_i(t)$ can be subsequently obtained as

$$z_i(t) = \frac{1}{2}\ln(\frac{\epsilon_i + \zeta_i(t)}{\bar{\epsilon}_i - \zeta_i(t)}) \tag{18}$$

with $\zeta_i(t) = e_{pi}(t)/\rho_i(t)$ being the normalized function.

Lemma 2 [13]: As long as the transformed error z_i is bounded, the MEMS gyroscope tracking error e_{pi} is within the preselected boundaries, i.e., $-\epsilon_i\rho_i(t) < e_{pi}(t) < \bar{\epsilon}_i\rho_i(t)$ always holds.

B. MLPNN

Considering the unknown time-varying disturbances imposed on the system, fast and accurate online disturbances identification is crucial for the performance of MEMS gyroscope. Thus, we employ RBFNN to approximate the lumped disturbances.

$$F_i = \omega_i^{*T}\boldsymbol{h}(\boldsymbol{x}_i) + \varepsilon_i \quad i = 1, 2 \tag{19}$$

where $\boldsymbol{x}_i = [x_{pi}, x_{vi}]^T$ represents the input matrix, ε_i is the approximation error and based on universal approximation theorem [32], [34], as long as the number of neural codes is large enough, there always exists an ideal value ω_i^* such that ε_i can be arbitrarily small and one always has

$$|\varepsilon_i| \le \bar{\varepsilon}_i \tag{20}$$

where $\bar{\varepsilon}_i$ is a positive constant.

As mentioned in *Remark* 1, the node number is required to be large enough to realize high-accuracy identification and consequently, the elements requiring to be adaptively updated will exponentially grow with node number, which will cause the issue of learning explosion. To reduce the learning dimension, a MLPNN technique is applied to reconstruct the lumped disturbances F_i, which is formulated as

$$F_i = \frac{1}{2}W_i^*||\boldsymbol{h}(\boldsymbol{x}_i)||2 + \varepsilon_i \quad i = 1, 2 \tag{21}$$

where $W_i^* = ||\omega_i^*||^2$ is defined as the norm of weight vector ω_i^*. Subsequently, we can easily obtain the approximation value of F_i, which is defined as

$$\hat{F}_i = \frac{1}{2}\hat{W}_i||\boldsymbol{h}(\boldsymbol{x}_i)||^2 \quad i = 1, 2 \tag{22}$$

where $\hat{W}$ is the estimation value of W^*, which can be produced via the following adaptive update law:

$$\dot{\hat{W}}_i = \Gamma_i(e_{vi}||\boldsymbol{h}(\boldsymbol{x}_i)||^2 - \kappa_i\hat{W}_i) \tag{23}$$

with e_{vi} denoting the tracking error of velocity subsystem, Γ_i being the adaptive gain, κ_i being a positive design parameter.

Remark 3: Using MLP technique, we only need to online update $\hat{W}_i$ rather than each element of $\hat{\boldsymbol{\omega}}_i$ like the works [19]–[21], such that the learning dimension is remarkably reduced, which greatly eases the computational burden without decreasing the identification accuracy.

C. QUANTIZEDCONTROL DESIGN

Inspired by the recursive controller design of backstepping control, MEMS gyroscope system is split up into two subsystems and accordingly, the controller design contains the following two parts.

STEP 1: Recollecting the transformed error $z_i(t)$ defined in (18), taking its time derivation produces

$$\begin{aligned}\dot{z}_i(t) &= \lambda_i(t)(\dot{e}_{pi}(t) - \dot{\rho}_i(t)e_{pi}(t)/\rho_i(t)) \\ &= \lambda_i(t)[x_{vi}(t) - \dot{x}_{pdi}(t) - \dot{\rho}_i(t)e_{pi}(t)/\rho_i(t)]\end{aligned} \tag{24}$$

with

$$\lambda_i(t) = \frac{1}{2\rho_i(t)}(\frac{1}{e_{pi}(t)/\rho_i(t) + \epsilon_i} - \frac{1}{e_{pi}(t)/\rho_i(t) - \bar{\epsilon}_i}) \tag{25}$$

To guarantee the tracking performance with prescribed UUB properties, the virtual control law is chosen as

$$\alpha_i(t) = -k_{1i}z_i(t) + \dot{x}_{pdi}(t) + \frac{\dot{\rho}_i(t)e_{pi}(t)}{\rho_i(t)}, \quad i = 1, 2 \tag{26}$$

where k_{1i} is the controller gain of position subsystem.

To avoid the issue of ''complexity explosion'' caused by analytical differentiation of $\alpha_i(t)$, we explore a first-order low-pass filter to obtain the time derivation of virtual control signal, which is formulated as

$$\tau_i\dot{\bar{\alpha}}_i + \bar{\alpha}_i = \alpha_i, \quad \bar{\alpha}_i(0) = \alpha_i(0), \ i = 1, 2 \tag{27}$$

with τ_i being the time delay constant of filter.

Define the filtering error σ_i as

$$\sigma_i = \bar{\alpha}_i - \alpha_i \tag{28}$$

Then, taking time derivative along (28) results in

$$\dot{\sigma}_i + \frac{\sigma_i}{\tau_i} = -\dot{\alpha}_i \tag{29}$$

and obviously

$$|\dot{\sigma}_i + \frac{\sigma_i}{\tau_i}| \le b_i(\ddot{x}_{pdi}, \dot{z}_i, e_{pi}, \dot{e}_{pi}, \rho_i, \dot{\rho}_i, \ddot{\rho}_i) \tag{30}$$

where $b_i(\ddot{x}_{pdi}, \dot{z}_i, e_{pi}, \dot{e}_{pi}, \rho_i, \dot{\rho}_i, \ddot{\rho}_i)$ is a continuous and smooth function satisfying $|b_i| \leq B_i$. Now, consider the following Lyapunov function candidate

$$V_{\sigma_i} = \frac{1}{2}\sigma_i^2 \tag{31}$$

Considering (29) and (30), we can obtain the time derivative of V_{σ_i}.

$$\dot{V}_{\sigma_i} = \dot{\sigma}_i\sigma_i \leq -\frac{\sigma_i^2}{\tau_i} + B_i\sigma_i \tag{32}$$

Based on Young's inequality, the following inequality holds.

$$B_i\sigma_i \leq \frac{1}{4}B_i^2 + \sigma_i^2 \tag{33}$$

Substituting (33) into (32) produces

$$\dot{V}_{\sigma_i} \leq (-\frac{1}{\tau_i} - 1)\sigma_i^2 + \frac{1}{4}B_i^2 \tag{34}$$

Simultaneously, considering (24), (26) and (28), $\dot{z}_i$ can be rewritten in the form of

$$\dot{z}_i = \lambda_i(-k_{1i}z_i + e_{vi} + \sigma_i) \tag{35}$$

Subsequently, consider the Lyapunov function candidate

$$V_{z_i} = \frac{z_i^2}{2\lambda_i} \tag{36}$$

Combined with (35), its time derivative is formulated as

$$\begin{aligned}\dot{V}_{z_i} &= \frac{z_i\dot{z}_i}{\lambda_i} - \frac{\dot{\lambda}_i}{2\lambda_i^2}z_i^2 \\ &= \frac{z_i}{\lambda_i}\lambda_i(-k_{1i}z_i + e_{vi} + \sigma_i) - \frac{\dot{\lambda}_i}{2\lambda_i^2}z_i^2 \\ &= -(k_{1i} + \frac{\dot{\lambda}_i}{2\lambda_i^2})z_i^2 + z_ie_{vi} + \sigma_iz_i\end{aligned} \tag{37}$$

With the aid of Young's inequality, we have

$$z_i\sigma_i \leq \frac{1}{4}z_i^2 + \sigma_i^2, \quad z_ie_{vi} \leq z_i^2 + \frac{1}{4}e_{vi}^2 \tag{38}$$

Substituting (38) into (37), $\dot{V}_{z_i}$ can be rewritten as

$$\dot{V}_{z_i} \leq (k_{1i} + \frac{\dot{\lambda}_i}{2\lambda_i^2} - \frac{5}{4})z_i^2 + \sigma_i^2 + \frac{1}{4}e_{vi}^2 \tag{39}$$

STEP 2: In this step, the actual control law is elaborated to eliminate the quantization error as well as ensure the UUB closed-loop stability of system. Firstly, we define the tracking error of MEMS gyroscope velocity subsystem as $e_{vi} = x_{vi} - \bar{\alpha}_i$. Next, using (4) and (6), its time derivative can be written as

$$\dot{e}_{vi} = F_i + \iota(u_i)u_i + T(u_i) - \dot{\bar{\alpha}}_i \tag{40}$$

Then, select the following Lyapunov function candidate

$$V_{e_{vi}} = \frac{1}{2}e_{vi}^2 \tag{41}$$

Based on (21) and (40), taking time derivative along (41) produces

$$\begin{aligned}\dot{V}_{e_{vi}} &= e_{vi}\dot{e}_{vi} \\ &= e_{vi}[F_i + \iota(u_i)u_i + T(u_i) - \dot{\bar{\alpha}}_i] \\ &= e_{vi}[\iota(u_i)u_i + T(u_i) + \frac{1}{2}W_i^*||\boldsymbol{h}(\boldsymbol{x}_i)||^2 + \varepsilon_i] - e_{vi}\dot{\bar{\alpha}}_i\end{aligned} \tag{42}$$

Define the auxiliary control signal υ_i as

$$\upsilon_i = k_{2i}e_{vi} + \frac{1}{2}\hat{W}_i||\boldsymbol{h}(\boldsymbol{x}_i)||^2 - \dot{\bar{\alpha}}_i \tag{43}$$

with k_{2i} being the controller gain of velocity subsystem.

To make up for the quantization error induced by LQ, adding and subtracting $e_{vi}\upsilon_i$, (42) can be rewritten in the following form

$$\begin{aligned}\dot{V}_{e_{vi}} &= e_{vi}\upsilon_i + e_{vi}[\iota(u_i)u_i + T(u_i) + \frac{1}{2}W_i^*||\boldsymbol{h}(\boldsymbol{x}_i)||^2 \\ &\quad + \varepsilon_i] - e_{vi}\dot{\bar{\alpha}}_i - e_{vi}\upsilon_i \\ &= e_{vi}\upsilon_i + e_{vi}[\iota(u_i)u_i + T(u_i)] + e_{vi}(\frac{1}{2}W_i^*||\boldsymbol{h}(\boldsymbol{x}_i)||^2 + \varepsilon_i) \\ &\quad - e_{vi}\dot{\bar{\alpha}}_i - e_{vi}(k_{2i}e_{vi} + \frac{1}{2}\hat{W}_i||\boldsymbol{h}(\boldsymbol{x}_i)||^2 - \dot{\bar{\alpha}}_i) \\ &= e_{vi}\upsilon_i + e_{vi}[\iota(u_i)u_i + T(u_i)] \\ &\quad + \frac{1}{2}e_{vi}\tilde{W}_i||\boldsymbol{h}(\boldsymbol{x}_i)||^2 - k_{2i}e_{vi}^2 + \varepsilon_ie_{vi}\end{aligned} \tag{44}$$

with $\tilde{W}_i = W_i^* - \hat{W}_i$ being the updating error.

Now, select the actual control law as

$$u_i = -\frac{e_{vi}\upsilon_i^2}{(1-\delta_i)\sqrt{e_{vi}^2\upsilon_i^2 + \beta_{1i}^2}} - \frac{e_{vi}u_{mi}}{(1-\delta_i)\sqrt{e_{vi}^2 + \beta_{2i}^2}} \tag{45}$$

where β_{1i}, β_{2i} are positive design parameters. With the aid of *Lemma* 1, we can easily obtain

$$e_{vi}\upsilon_i + e_{vi}[\iota(u_i)u_i + T(u_i)] \leq e_{vi}[(1+\delta_i)u_i + u_{mi}] + e_{vi}\upsilon_i \tag{46}$$

Meanwhile, the following inequalities apparently hold

$$\begin{aligned}-\frac{e_{vi}^2\upsilon_i^2}{\sqrt{e_{vi}^2\upsilon_i^2 + \beta_{1i}^2}} &\leq -\frac{(e_{vi}\upsilon_i)^2}{|e_{vi}\upsilon_i| + \beta_{1i}} < -\frac{(e_{vi}\upsilon_i)^2 - \beta_{1i}^2}{|e_{vi}\upsilon_i| + \beta_{1i}} \\ &\leq \beta_{1i} - e_{vi}\upsilon_i \\ -\frac{e_{vi}^2}{\sqrt{e_{vi}^2 + \beta_{2i}^2}} &\leq -\frac{e_{vi}^2}{|e_{vi}| + \beta_{2i}} < -\frac{e_{vi}^2 - \beta_{2i}^2}{|e_{vi}| + \beta_{2i}} \\ &\leq \beta_{2i} - e_{vi}\end{aligned} \tag{47}$$

Then (46) can be further rewritten in the following concise form

$$e_{vi}\upsilon_i + e_{vi}[\iota(u_i)u_i + T(u_i)] \leq \beta_{1i} + u_{mi}\beta_{2i} \tag{48}$$

Substituting (48) into (44), $\dot{V}_{e_{vi}}$ can be finally written as

$$\dot{V}_{e_{vi}} \leq \beta_{1i} + u_{mi}\beta_{2i} + \frac{1}{2}e_{vi}\tilde{W}_i||\boldsymbol{h}(\boldsymbol{x}_i)||^2 - k_{2i}e_{vi}^2 + \varepsilon_ie_{vi} \tag{49}$$

IV. PERFORMANCE ANALYSIS

Theorem 1: Consider the MEMS gyroscope model (4), the control signals (45), the virtual control law (26), the adaptive update law (23) and DSC (27). For any bounded initial conditions satisfying $-\epsilon_i\rho_i(0) < e_{pi}(0) < \bar{\epsilon}_i\rho_i(0)$, $i = 1, 2$, there always exist constants defined by (54), such that all the involved signals in MEMS gyroscope system converge to small residual sets and the prescribed tracking performance, i.e., $-\epsilon_i\rho_i(t) < e_{pi}(t) < \bar{\epsilon}_i\rho_i(t)$ can be satisfied.

Proof: Choose the overall Lyapunov function candidate as:

$$V = \sum_{i=1}^{2}[V_{\sigma_i} + V_{z_i} + V_{e_{vi}} + V_{\tilde{W}_i}] = \sum_{i=1}^{2}[\frac{1}{2}\sigma_i^2 + \frac{z_i^2}{2\lambda_i} + \frac{1}{2}e_{vi}^2 + \frac{1}{2\Gamma_i}\tilde{W}_i^2] \tag{50}$$

With the aid of (34), (39) and (49), taking time derivative along with (50) produces

$$\dot{V} \le \sum_{i=1}^{2}[(-\frac{1}{\tau_i} - 1)\sigma_i^2 + \frac{1}{4}B_i^2 + (k_{1i} + \frac{\dot{\lambda}_i}{2\lambda_i^2} - \frac{5}{4})z_i^2 + \sigma_i^2 + \frac{1}{4}e_{vi}^2\beta_{1i} + u_{mi}\beta_{2i} + \frac{1}{2}e_{vi}\tilde{W}_i||\boldsymbol{h}(\boldsymbol{x}_i)||^2 - k_{2i}e_{vi}^2 + \varepsilon_i e_{vi} + \frac{\tilde{W}_i\dot{\tilde{W}}_i}{\Gamma_i}] \tag{51}$$

Recalling the definition of updating error $\tilde{W}_i$, using Young's inequality, the following inequalities can be obtained

$$\kappa_i\hat{W}_i\tilde{W}_i \le \kappa_i(-\frac{\tilde{W}_i}{2} + \frac{W_i^{*2}}{2}), \quad \varepsilon_i e_{vi} \le \frac{1}{4}\bar{\varepsilon}_i^2 + e_{vi}^2$$
$$e_{vi}\tilde{W}_i||\boldsymbol{h}(\boldsymbol{x}_i)||^2 \le \frac{1}{2}e_{vi}^2||\boldsymbol{h}(\boldsymbol{x}_i)||^2 + \frac{1}{2}\tilde{W}_i^2||\boldsymbol{h}(\boldsymbol{x}_i)||^2 \tag{52}$$

With the aid of (23) and (52), (50) can be further rewritten as

$$\dot{V} \le \sum_{i=1}^{2}[-(\frac{1}{\tau_i} - 2)\sigma_i^2 - (k_{1i} + \frac{\dot{\lambda}_i}{2\lambda_i^2} - \frac{5}{4})z_i^2 - (k_{2i}e_{vi}^2 - \frac{1}{4}\beta_{1i} - \frac{1}{4}||\boldsymbol{h}(\boldsymbol{x}_i)||^2 - 1)e_{vi}^2 - (\frac{\kappa_i}{2} - \frac{1}{4}||\boldsymbol{h}(\boldsymbol{x}_i)||^2)\tilde{W}_i^2 + \frac{1}{4}B_i^2 + u_{mi}\beta_{2i} + \frac{1}{4}\bar{\varepsilon}_i^2 + \frac{\kappa_i W_i^{*2}}{2}] \tag{53}$$

Then, from (53), we can easily obtain that if the following inequalities

$$\begin{cases} \frac{1}{\tau_i} - 2 \ge \frac{K}{2} \\ k_{1i} + \frac{\dot{\lambda}_i}{2\lambda_i^2} - \frac{5}{4} \ge \frac{K}{2\lambda_i} \\ k_{2i}e_{vi}^2 - \frac{1}{4}\beta_{1i} - \frac{1}{4}||\boldsymbol{h}(\boldsymbol{x}_i)||^2 - 1 \ge \frac{K}{2\Gamma_i} \\ \frac{\kappa_i}{2} - \frac{1}{4}||\boldsymbol{h}(\boldsymbol{x}_i)||^2 \ge \frac{K}{2} \end{cases} \tag{54}$$

hold, it can be derived that

$$\dot{V} \le -KV + C \tag{55}$$

with C being a positive constant defined as

$$C = \sum_{i=1}^{2}[\frac{1}{4}B_i^2 + u_{mi}\beta_{2i} + \frac{1}{4}\bar{\varepsilon}_i^2 + \frac{\kappa_i W_i^{*2}}{2}] \tag{56}$$

The initial conditions are all bounded, so we can make a feasible assumption that $V(0) = A$. Subsequently, as long as $K > C/A$ holds, we can draw the conclusion that $\forall t > 0$, $\dot{V}(t) \le 0$, in other word, $V(t) \le A$ always holds. Hence, the signals involved in closed-loop system are all UUB and meanwhile, with the aid of *Lemma* 2, it can be discovered that tracking error e_{pi} always falls into the prescribed boundary, such that Theorem 1 is eventually proved.

V. SIMULATION RESULTS

To validate the effectiveness of our proposed control method, several simulations are performed via MATLAB/SIMULINK. Firstly, the physical parameters of MEMS gyroscope, borrowed from [4], are chosen as

$$m = 1.8\times10^{-7}kg, \quad k_{xx}=63.955N/m, \quad k_{yy}=95.92N/m,$$
$$k_{xy} = 12.779N/m, \quad d_{xx} = 1.8\times10^{-6}Ns/m$$
$$d_{yy} = 1.8\times10^{-6}Ns/m, \quad d_{xy} = 3.6\times10^{-7}Ns/m \tag{57}$$

Subsequently, the non-dimensional parameters can be calculated as

$$k_x^2 = 355.3, \quad k_y^2 = 355.3, \quad k_{xy} = 70.99$$
$$D_x = 0.01, \quad D_y = 0.01, \quad D_{xy} = 0.002, \quad \Omega_z = 0.1 \tag{58}$$

The reference trajectory of displacements is chosen as

$$\boldsymbol{x}_{pd}(t) = \begin{bmatrix} sin(4.17t) \\ 0 \end{bmatrix}, \quad t \ge 0 \tag{59}$$

Choose the external disturbances $\boldsymbol{\xi}$ as

$$\boldsymbol{\xi} = \begin{bmatrix} 20\cos(30t) + 30\sin(20t) \\ 10\cos(40t) + 20\sin(20t) \end{bmatrix}, \quad t \ge 0 \tag{60}$$

TABLE 1 lists the design parameters of the presented controller.

TABLE 1. Parameters for the proposed control algorithm.

Section	Parameters
PPC	$l_1 = l_2 = 20, \rho_{1\infty} = 0.15, \rho_{2\infty} = 0.1$
	$\rho_{10} = 1.1, \rho_{20} = 0.8, \bar{c}_1 = 1, \bar{c}_2 = 0.9, \underline{c}_1 = 1, \underline{c}_2 = 0.9$
LQ	$u_{m1} = u_{m2} = 0.5, \delta_1 = \delta_2 = 0.9, N = 91$
MLPNN	$c_{jk} = 0.1, \quad b = 1.5, \quad n = 10$
	$\kappa_1 = 0.1056, \kappa_2 = 0.0568, \Gamma_1 = 1800, \Gamma_2 = 1850$
DSC	$\tau_1 = \tau_2 = 0.05$
Controller	$k_{11} = k_{12} = 150, k_{21} = 80, k_{22} = 150$
	$\beta_{11} = \beta_{12} = 10, \beta_{21} = \beta_{22} = 20$

A. EFFECTIVENESS ANALYSIS

Using the parameters given above, the first simulation is conducted to validate the effectiveness of proposed control schemes, where the initial conditions of MEMS gyroscope are chosen as $x_p(0) = [-0.9, 0.5]^T, x_v(0) = [0, 0]^T$. The simulation results are depicted in Figs. 3-6 and obviously, both transient overshoots and steady-state maximum tracking error are restricted to predetermined small values, such that guaranteed tracking performance can be obtained via appropriately selecting performance functions. Furthermore, the convergence rate is very fast, as can be seen from Fig. 3, only after 0.08s, both tracking error of position and velocity subsystem coincide with the reference trajectory perfectly. Meanwhile, the quantization performance is clearly reflected from Fig. 6, where the continuous input signal is converted to the one taking values in finite sets, such that the issue of actuator limitation is eliminated and data size requiring to be transmitted is remarkably lessened. Although the precision of input signal is notably reduced, high-accuracy tracking performance as well as identification of uncertainties can still be available, which is mainly attributed to the effective error compensation methodology and PPC technique.

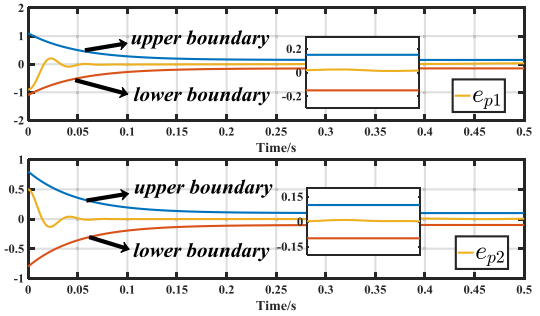

FIGURE 3. Tracking error of position subsystem.

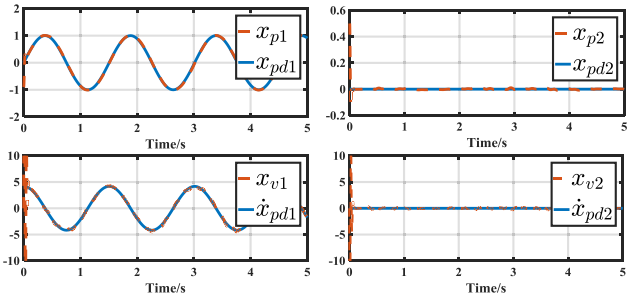

FIGURE 4. Tracking performance.

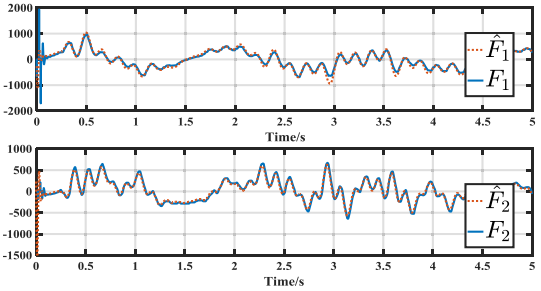

FIGURE 5. Uncertainties identification.

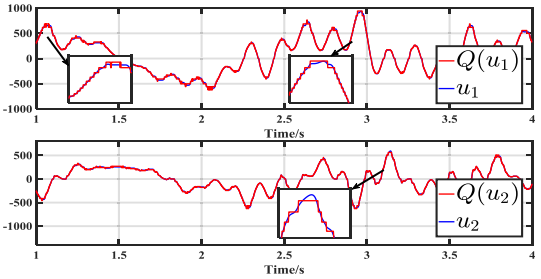

FIGURE 6. Quantization performance.

B. COMPARATIVE SIMULATIONS

To further demonstrate the superiorities of our proposed control method over existing ones, some comparative simulations are performed and presented in this section. Firstly, the simulations among proposed control scheme, backstepping control [7] are given in Fig. 7. In light of the fairness, we apply these algorithms with the same control parameters.

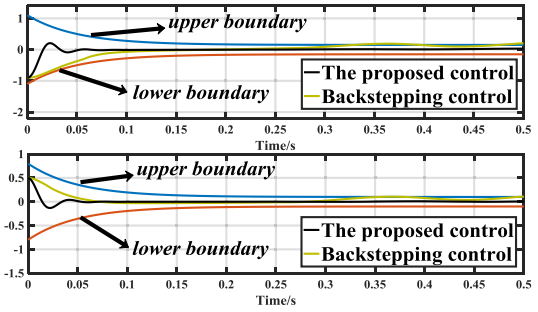

FIGURE 7. Comparative simulations between the proposed control and backstepping control [7].

TABLE 2. Comparisons between the proposed control and the one free of LQ.

Index		Without LQ	The Proposed Scheme	Variation
Data Size	u_1	10000	1559	-84.41%
	u_2	10000	2547	-74.53%
Steady Tracking Accuracy (Standard Deviation)	e_{p1}	0.0194	0.0195	0.51%
	e_{p2}	0.0075	0.0075	-

TABLE 3. Comparisons between RBFNN and MLPNN.

Index		RBFNN	MLPNN	Variation
Average Computation Time	$\hat{F}_1$	1.216ms	0.128ms	-88.24%
	$\hat{F}_2$	1.219ms	0.137ms	-88.76%
Steady Identification Accuracy (Standard Deviation)	$\tilde{F}_1$	6.43	6.43	-
	$\tilde{F}_2$	3.86	3.86	-

TABLE 4. Comparisons among our control Method and Existing Ones.

Comparison	Sliding-mode control schemes in [37]-[39]	Backstepping control schemes in [40]	Quantized control schemes schemes in [41], [42]	Our control scheme
The studied problem	Anti-disturbance	Anti-disturbance	Anti-disturbance and resource limitation	Anti-disturbance, resource limitation, and computation burden
The considered system	MEMS gyroscope	Micro gyroscope	Nonlinear system	MEMS gyroscope
The issue of learning explosion	Existing	Existing	Existing	Avoided
Resource limitation	Not studied	Not studied	Studied under the assumption that input signals are bounded.	Studied without such assumption.

The results clearly indicate that both transient and steady-state tracking performance of the proposed algorithm are much better than that of backstepping control. In addition, the proposed method performs faster convergence rate of tracking error by virtue of performance boundaries and effective error transformation mechanism.

In addition, to further clarify the remarkable quantization performance, a statistic with respect to data size of input signal as well as tracking accuracy is presented in TABLE 2, from which we can discover that with the aid of LQ as well as effective error compensation mechanism, the data amount of control input required to be transmitted is notably reduced while the steady tracking accuracy is almost the same as the case without LQ, such that the compromise between tracking performance and actuator bandwidth can be finally obtained.

Furthermore, aiming at testifying the superiorities of MLPNN in terms of computational burden and tracking accuracy, we conduct the comparative simulations between MLPNN and RBFNN [34], the simulation results are demonstrated in TABLE 3, where the average computation time denotes the average time of updating of each neural weight. It can be easily discovered that the heavy computation burden of RBFNN appears due to the learning process of each element of neural weight vectors. Evidently, the computation time of RBFNN is much longer than MLPNN as the nodes number further improves. While with the aid of MLPNN, we can achieve almost the same accurate identification results with much slighter computation load.

VI. CONCLUSION

In this paper, we propose a MLP-based neural control for MEMS gyroscope with guaranteed performance and quantized input. Firstly, we employ a LQ to generate input signal for MEMS gyroscope, the issues of actuator bandwidth and communication resource constraints are effectively eliminated. Considering the quantization error imposing on MEMS gyroscope system, a PPC technique is employed to realize guaranteed tracking performance in the existence of uncertainties. In addition, MLPNN is utilized to realize high-accuracy identification of lumped disturbances with slight computational burden. In the near future, we will focus on an event-triggered fuzzy control scheme with full-state constraints in pursuit of reliable operation of MEMS gyroscope with resource limitation.

APPENDIX

See Table 4.

ACKNOWLEDGMENT

The authors would like to express sincere gratitude to the anonymous reviewers and the editor for their precious remarks and advices, which will significantly improve the quality of their paper.

REFERENCES

[1] Y. Ren, X. Chen, Y. Cai, H. Zhang, C. Xin, and Q. Liu, "Attitude-rate measurement and control integration using magnetically suspended control and sensitive gyroscopes," *IEEE Trans. Ind. Electron.*, vol. 65, no. 6, pp. 4921–4932, Jun. 2018.

[2] G. Wu, B. Han, D. D. Cheam, L. C. Wai, P. H. K. Chang, N. Singh, and Y. Gu, "Development of six-degree-of-freedom inertial sensors with an 8-in advanced MEMS fabrication platform," *IEEE Trans. Ind. Electron.*, vol. 66, no. 5, pp. 3835–3842, May 2019.

[3] Q. Zheng, L. Dong, D. Hui Lee, and Z. Gao, "Active disturbance rejection control for MEMS gyroscopes," *IEEE Trans. Control Syst. Technol.*, vol. 17, no. 6, pp. 1432–1438, Nov. 2009.

[4] H. Wang, L. Hua, Y. Guo, and C. Lu, "Control of Z-axis MEMS gyroscope using adaptive fractional order dynamic sliding mode approach," *IEEE Access*, vol. 7, pp. 133008–133016, 2019.

[5] Y. Chu, J. Fei, and S. Hou, "Adaptive neural backstepping PID global sliding mode fuzzy control of MEMS gyroscope," *IEEE Access*, vol. 7, pp. 37918–37926, 2019.

[6] R. Zhang, T. Shao, W. Zhao, A. Li, and B. Xu, "Sliding mode control of MEMS gyroscopes using composite learning," *Neurocomputing*, vol. 275, pp. 2555–2564, Jan. 2018.

[7] J. Fei and X. Liang, "Adaptive backstepping fuzzy neural network fractional-order control of microgyroscope using a nonsingular terminal sliding mode controller," *Complexity*, vol. 2018, Sep. 2018, Art. no. 5246074.

[8] M. Rahmani, "MEMS gyroscope control using a novel compound robust control," *ISA Trans.*, vol. 72, pp. 37–43, Jan. 2018.

[9] B. Xu, R. Zhang, S. Li, W. He, and Z. Shi, "Composite neural learning-based nonsingular terminal sliding mode control of MEMS gyroscopes," *IEEE Trans. Neural Netw. Learn. Syst.*, to be published.
[10] J. Zhou, C. Wen, W. Wang, and F. Yang, "Adaptive backstepping control of nonlinear uncertain systems with quantized states," *IEEE Trans. Autom. Control*, vol. 64, no. 11, pp. 4756–4763, Nov. 2019.
[11] S. A. Karthick, R. Sakthivel, Y. K. Ma, S. Mohanapriya, and A. Leelamani, "Disturbance rejection of fractional-order T-S fuzzy neural networks based on quantized dynamic output feedback controller," *Appl. Math. Comput.*, vol. 361, pp. 846–857, Nov. 2019.
[12] L. Li, P. Shi, Y. Zhao, D. Zhou, and W. Xing, "Containment control of multi-agent systems with uniform quantization," *Circuits Syst. Signal Process.*, vol. 38, no. 9, pp. 3952–3970, Sep. 2019.
[13] Q. Guo, Y. Zhang, B. G. Celler, and S. W. Su, "Neural adaptive backstepping control of a robotic manipulator with prescribed performance constraint," *IEEE Trans. Neural Netw. Learn. Syst.*, vol. 30, no. 12, pp. 3572–3583, Dec. 2019.
[14] C. Xi and J. Dong, "Adaptive fuzzy guaranteed performance control for uncertain nonlinear systems with event-triggered input," *Appl. Math. Comput.*, vol. 363, Dec. 2019, Art. no. 124604.
[15] X. Wang, Q. Wu, and X. Yin, "Adaptive finite-time prescribed performance control of switched nonlinear systems with unknown actuator dead-zone," *Int. J. Syst. Sci.*, vol. 51, no. 1, pp. 133–145, Jan. 2020.
[16] C. Xu, H. Lei, and N. Lu, "Active disturbance rejection control for air-breathing hypersonic vehicles based on prescribed performance function," *Int. J. Aerosp. Eng.*, vol. 2019, Nov. 2019, Art. no. 4129136.
[17] Y. Wang and J. Hu, "Improved prescribed performance control for air-breathing hypersonic vehicles with unknown deadzone input nonlinearity," *ISA Trans.*, vol. 79, pp. 95–107, Aug. 2018.
[18] Z. Peng, J. Wang, and J. Wang, "Constrained control of autonomous underwater vehicles based on command optimization and disturbance estimation," *IEEE Trans. Ind. Electron.*, vol. 66, no. 5, pp. 3627–3635, May 2019.
[19] G. Gao, J. Wang, and X. Wang, "Prescribed-performance fault-tolerant control for feedback linearisable systems with an aircraft application," *Int. J. Control*, vol. 90, no. 5, pp. 932–949, May 2017.
[20] X. Shao, J. Liu, H. Cao, C. Shen, and H. Wang, "Robust dynamic surface trajectory tracking control for a quadrotor UAV via extended state observer," *Int. J. Robust. Nonlinear Control*, vol. 28, no. 7, pp. 2700–2719, May 2018.
[21] S. Xingling, T. Biao, Y. Wei, and Z. Wendong, "Estimator-based MLP neuroadaptive dynamic surface containment control with prescribed performance for multiple quadrotors," *Aerosp. Sci. Technol.*, vol. 97, Feb. 2020, Art. no. 105620.
[22] Y. Zhang, D. Wang, and Z. Peng, "Consensus maneuvering for a class of nonlinear multivehicle systems in strict-feedback form," *IEEE Trans. Cybern.*, vol. 49, no. 5, pp. 1759–1767, May 2019.
[23] D. Li, C. L. P. Chen, Y.-J. Liu, and S. Tong, "Neural network controller design for a class of nonlinear delayed systems with time-varying full-state constraints," *IEEE Trans. Neural Netw. Learn. Syst.*, vol. 30, no. 9, pp. 2625–2636, Sep. 2019.
[24] M. Xia and T. Zhang, "Adaptive neural dynamic surface control for full state constrained stochastic nonlinear systems with unmodeled dynamics," *J. Franklin Inst.*, vol. 356, no. 1, pp. 129–146, Jan. 2019.
[25] X. Xia and T. Zhang, "Robust adaptive quantized DSC of uncertain pure-feedback nonlinear systems with time-varying output and state constraints," *Int. J. Robust. Nonlinear Control*, vol. 28, no. 10, pp. 3357–3375, Jul. 2018.
[26] X. Shao, L. Wang, J. Li, and J. Liu, "High-order ESO based output feedback dynamic surface control for quadrotors under position constraints and uncertainties," *Aerosp. Sci. Technol.*, vol. 89, pp. 288–298, Jun. 2019.
[27] X. Shao, N. Liu, Z. Wang, W. Zhang, and W. Yang, "Neuroadaptive integral robust control of visual quadrotor for tracking a moving object," *Mech. Syst. Signal Process.*, vol. 136, Feb. 2020, Art. no. 106513.
[28] Y. Fang, D. Lei, and J. Fei, "Adaptive double neural network control for micro-gyroscope based on dynamic surface controller," *Adv. Mech. Eng.*, vol. 11, no. 2, Feb. 2019, Art. no. 168781401982715.
[29] J. Hu, X. Sun, S. Liu, and L. He, "Adaptive finite-time formation tracking control for multiple nonholonomic UAV system with uncertainties and quantized input," *Int. J. Adapt. Control Signal Process.*, vol. 33, no. 1, pp. 114–129, Jan. 2019.
[30] M. Hosseini-Pishrobat and J. Keighobadi, "Robust output regulation of a triaxial MEMS gyroscope via nonlinear active disturbance rejection," *Int. J. Robust. Nonlinear Control*, vol. 28, no. 5, pp. 1830–1851, Mar. 2018.
[31] X. Bu, X. Wu, F. Zhu, J. Huang, Z. Ma, and R. Zhang, "Novel prescribed performance neural control of a flexible air-breathing hypersonic vehicle with unknown initial errors," *ISA Trans.*, vol. 59, pp. 149–159, Nov. 2015.
[32] W. R. Mendes, F. M. U. Araújo, R. Dutta, and D. M. Heeren, "Fuzzy control system for variable rate irrigation using remote sensing," *Expert Syst. Appl.*, vol. 124, pp. 13–24, Jun. 2019.
[33] Z. Peng, J. Hu, K. Shi, R. Luo, R. Huang, B. K. Ghosh, and J. Huang, "A novel optimal bipartite consensus control scheme for unknown multi-agent systems via model-free reinforcement learning," *Appl. Math. Comput.*, vol. 369, Mar. 2020, Art. no. 124821.
[34] Y. Chu, Y. Fang, and J. Fei, "Adaptive neural dynamic global PID sliding mode control for MEMS gyroscope," *Int. J. Mach. Learn. Cyber.*, vol. 8, no. 5, pp. 1707–1718, Oct. 2017.
[35] Y. Shi, X. Shao, and W. Zhang, "Quantized learning control for flexible air-breathing hypersonic vehicle with limited actuator bandwidth and prescribed performance," *Aerosp. Sci. Technol.*, vol. 97, Feb. 2020, Art. no. 105629.
[36] X. Shao and Y. Shi, "Neural adaptive control for MEMS gyroscope with full-state constraints and quantized input," *IEEE Trans. Ind. Informat.*, to be published, doi: 10.1109/TII.2020.2968345.
[37] Y. Fang, J. Fei, and D. Cao, "Adaptive fuzzy-neural fractional-order current control of active power filter with finite-time sliding controller," *Int. J. Fuzzy Syst.*, vol. 21, no. 5, pp. 1533–1543, Jul. 2019.
[38] J. Fei and Z. Feng, "Adaptive fuzzy super-twisting sliding mode control for microgyroscope," *Complexity*, vol. 2019, Feb. 2019, Art. no. 6942642, doi: 10.1155/2019/6942642.
[39] J. Fei and Y. Chu, "Double hidden layer output feedback neural adaptive global sliding mode control of active power filter," *IEEE Trans. Power Electron.*, vol. 35, no. 3, pp. 3069–3084, Mar. 2020.
[40] Y. Fang, J. Fei, and Y. Yang, "Adaptive backstepping design of a microgyroscope," *Micromachines*, vol. 9, no. 7, p. 338, Jul. 2018.
[41] W. Khan, Y. Lin, S. U. Khan, and N. Ullah, "Adaptive output-feedback control for a class of nonlinear systems with actuator failures and input quantisation," *Int. J. Control*, vol. 92, no. 7, pp. 1609–1619, Jul. 2019.
[42] W. Khan, Y. Lin, S. U. Khan, and N. Ullah, "Quantized adaptive decentralized control for interconnected nonlinear systems with actuator faults," *Appl. Math. Comput.*, vol. 320, pp. 175–189, Mar. 2018.

HAONAN SI was born in Jiangsu, China, in 1998. He is currently pursuing the B.Sc. degree in communication with the North University of China. His current research interests contain quantized control, constrained control, and neural learning control.

XINGLING SHAO received the M.S. degree in instrument science and technology from the North University of China, Shanxi, China, in 2012, and the Ph.D. degree in navigation, guidance and control from Beihang University, Beijing, China, in 2016. Since 2018, he has been a Professor with the Department of Instrument and Electronics, North University of China. His current research interests are in the fields of anti-disturbance control theory and application for nonlinear uncertain systems, advanced signal processing methods for navigation, and robust cooperative flight control theory and method for quadrotors.

WENDONG ZHANG was born in Henan, China, in 1962. He is currently a Professor with the School of Instrument and Electronics, North University of China, Taiyuan, China. His research interest includes dynamics testing and control theory for nonlinear uncertain systems.